QUANTITATIVE 3D-ANALYSIS OF THE TRANSLABYRINTHINE APPROACH AND THE SIGMOID SINUS:

A cadaveric study applying three-dimensional visualization and modelling.

Summary

This document presents the results of a 12-week research internship at the department of Otorhinolaryngology in Utrecht. It investigates the ancillary exposure granted by compression of the sigmoid sinus during lateral skull base surgery with the use of cadaveric specimens and 3D modelling. Results show that in 40% of the cases the provided exposure while merely retracting instead of collapsing this sinus is equal or greater than 50% of other cases in which the sinus is collapsed. It is therefore concluded that with careful patient selection a translabyrinthine resection in which the sigmoid sinus is not compressed, is feasible while providing sufficient exposure. Further research is necessary to evaluate if this manoeuvre is translatable to patient care, and if it will reduce sinus related morbidity as hypothesized.

Author: Djenghiz P.S. Samlal, BSc, MA
Student number: 5842646
Supervisor: H.G.X.M. Thomeer, MD, PhD
Department: Otorhinolaryngology, Skull Base Department, UMCU, The Netherlands.

Period: 26/06/2024 (wk26) - 15/09/2024 (wk37)
Word count (main text, excl. references, tables, figures): 4354

0. Abstract

Introduction: Perioperative sigmoid sinus compression and sinus injury might be associated with various post-operative complication (e.g., CFS leakage, headache, intracranial hypertension, cerebellar infarct). This study was designed to quantify the effect of the sigmoid sinus (SS) on the operative exposure obtained in the translabyrinthine approach. Furthermore, it quantifies the ancillary exposure due to retraction of a skeletonized sinus. It is hypnotized that in selected cases a dorsally mobilized skeletonized SS will provide sufficient exposure to perform a translabyrinthine resection of cerebellopontine angle tumours.

Method: Twelve translabyrinthine proper approaches were performed on fresh frozen cadaveric heads. The position of the sigmoid sinus was varied in three procedures: stationary (TL-S), posterior retraction (TL-R), and collapsing of the sinus (TL-C). Based on the post-operative CT-scans, a high-definition 3D reconstruction of the visualize the resection cavity was obtained. The primary outcome, 'surgical freedom' (mm^2), was the area at the level of the craniotomy from which the internal acoustic porus could be reached in an obstructed straight line. Secondary outcomes include the 'exposure angle' (degrees), 'angle of attack' (degrees) and pre-sigmoid depth (mm^2).

Results: When retraction of the SS was performed during TL-R, surgical freedom increased by a mean of 41% (range: 9-92%, SD: 28) when compared to no retraction (TL-S). Collapsing the SS in TL-C provided a mean increase of 52% (range: 19-95%, SD: 22) compared to TL-S. In some specimens, the TL-R provided a greater surgical freedom than the TL-C; however, on average an increase of 10% (range: -10–30%, SD: 12) in favour of the TL-C is observed when compared to TL-R. In most cases the exposure is the greatest when the sigmoid sinus is collapsed. However, in 40% of the specimens the provided exposure while retracting (TL-R) instead of collapsing (TL-S) this sinus is equal or greater than 50% of other specimens in which the sinus is collapsed.

Conclusion: It is concluded that in cases with favourable anatomy, the translabyrinthine resection while retracting a skeletonized sinus provides sufficient exposure to the cerebellopontine angle. However, further research is necessary to evaluate the translatability of manoeuvre from cadaveric specimens to a clinical setting.

Keywords: Skull Base, Microsurgery, Cerebellopontine, Vestibular Schwannoma, 3D modelling, Quantitative Anatomy.

Abbreviations

SS = sigmoid sinus, ICA = internal auditory canal, CPA = cerebellopontine angle, TL = translabyrinthine proper approach, TL-S = stationary sinus, TL-R = retracted sinus, TL-C = collapsed sinus, SF = surgical freedom, EA = exposure angle, AA = angle of attack.

1. Introduction

During the past decades, an increased attention has been paid to quantify the additional exposure gained through various modified skull base techniques compared to traditional approaches (1-5). Furthermore, there is a trend in preferences towards minimally invasive, and endoscopic skull base surgery (6-10). These research lines have clinical relevance owing to their potential to save unnecessary elongation of operative time and associated morbidity, by informing the multidisciplinary surgical team about the expected exposure. Furthermore, it can aid in selection of patients whose favourable anatomy permits a more reserved bony resection while still granting satisfactory exposure to the internal auditory canal (IAC) and cerebellopontine angle (CPA) (4, 5). An appreciable proportion of this literature has focused on the orbitozygomatic and pterional approaches (1, 2, 11-15). However, quantitative anatomical studies on pre-sigmoid (petrous) approaches remain relatively scares (3-5, 16-18). This study, therefore, intent to add to the existing body of knowledge, quantitative information about this complex though rewarding anatomical corridor, while using a synthesis of cadaveric specimens on which the procedure is performed and a 3D-reconstruction of it in pursuance of meticulous measurements.

Hoz et al. (2023) recently proposed a classification system of these pre-sigmoid approaches based on relevant surgical anatomy, differentiating 5 translabyrinthine (anterior) and 4 retrolabyrinthine (posterior) approaches (19). These approaches are mainly used in vestibular Schwannoma and petroclival/CPA meningioma resection; however, indication for these approaches extent to amongst others petrous apex granuloma, chondrosarcoma, pontine cavernoma, vestibular neurectomy and basilar artery aneurysms (19). While this study will focus on the translabyrinthine proper approach as defined by Hoz et al. (hereafter: TL), general lessons are likely transferable to the other pre-sigmoid petrosal approaches. *Figure 1* shows the provide exposure during TL resection.

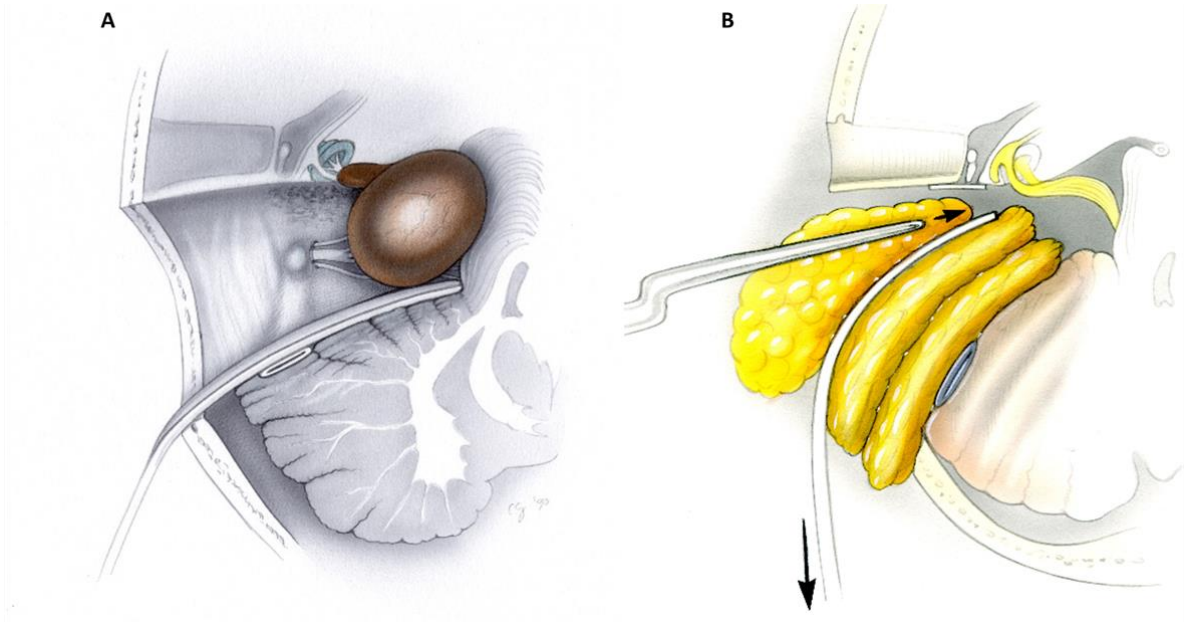

Figure 1: Transversal schematic view of the provide exposure in the CPA during translabyrinthine resection of a Schwannoma (A) and closure of this cavity using fat grafts (B). Note that the sigmoid sinus is fully compressed underneath the retractor and fat grafts. *Permission granted by RK Jackler for the non-profit educational use of this image* (20).

In the TL approach, both prolonged sinus retraction during surgery as well as pressure caused by fat-grafts in the resection cavity after closure, can cause compression of the sigmoid sinus (SS), which

might increase post-operative morbidity (e.g. CFS leakage, headache, intracranial hypertension, cerebellar infarct) (21-25). Furthermore, SS injury (e.g., during routine de-skeletonization) can lead to SS embolization and even pulmonary embolism (22). If this is the case, an increase in SS related morbidity is hypothesized when compared to retrosigmoid resection of CPA tumours, throughout which neither the sinus is retracted, nor are compressive fat-grafts used during closure. Comparative studies on the incidence of SS related morbidity after CPA tumour resection stratified by pre-sigmoid (e.g. TL) and retrosigmoid approaches remain scares; results trend towards an increased incidence after pre-sigmoid resection, however in not all studies significancy was reached (25-27). A systematic review and meta-analysis is recommended to further test this the hypothesis.

Nonetheless it might, in addition to a possible decrease in SS associated complications, be beneficial to analyse the feasibility of a TL-approach in which the SS remains patent by leaving it skeletonized, instead of ridding it of its bony protection. In selective cases, with favourable anatomy (e.g., large Trautmann's area, dorsally located slender sinus, limited extension of the tumour in the internal auditory canal), it might be time and cost saving to withhold further dissection of the sinus for marginal gains in exposure. It is deemed a good maxim to withhold those procedure that offer insignificant benefits.

No previous quantitative analysis has been found that compared the effect of increasing SS retraction on the ancillary exposure gained by this manoeuvre during translabyrinthine resection of cerebellopontine angle tumours. The primary aim of this study is therefore to provide a quantification of the additional exposure gained due to retraction of a de-skeletonized SS compared to the provided exposure of a skeletonized SS in its natural position. Secondary, it will assess the feasibility and quantification of dorsally mobilizing a skeletonized SS, in order to increase exposure while maintaining patency through and protection of the sinus. It is hypothesized that in specifically selected cases a dorsally mobilized skeletonized SS will provide sufficient exposure to perform a translabyrinthine resection of CPA tumours.

2. Materials and Methods

2.1. Specimen preparation and setting

Six fresh frozen non-fixated non-latex-perfused cadaveric heads were used to perform a total of 12 temporal bone dissection on both the right and left sides. Preservation of the specimens during the duration of experiments was achieved by (re-)freezing them to -19 ^{o}C, and only locally thawing the area of interest under continuous irrigation during dissection. All procedures concerned the translabyrinthine proper approach with various displacement of the sigmoid sinus: TL-stationary sinus (TL-S), TL-retracted sinus (TL-R), TL-collapsed sinus (TL-C). Dissection was performed by a single medical student (D.S.) and validated by a senior neurotologist-skull base surgeon (H.T.). Optical magnification (3x to 40x) was achieved under an operating microscope. After each procedure the specimen was refrozen. High-resolution cone beam CT scans (scan window 12x8cm; contiguous non-overlapping slices) were obtained pre-operatively and after each procedure.

Raw data from the scans were semi-automatically segmented based on their Hounsfield unit and voxel location and converted to a three-dimensional object with Materialise Mimics 24.0, 3D medical image segmentation software (Materialise NV, Leuven, Belgium). Further manipulation and analysis of this 3D-model took place in Materialise 3-Matic 17.0, Design optimization software (Materialise NV, Leuven, Belgium).

2.2. Surgical procedures

The three procedures were performed progressing sequentially from the least to the most extensive one: TL-S → TL-R → TL-C. The translabyrinthine proper approach was attempted during the first procedure (TL-S), working between the skeletonized SS and fascial nerve (19). A thin bony covering was conserved over the dura and IAC to improve its radiopacity. To perform dorsal retraction of the skeletonized sinus during the TL-R, up to 20 mm of retro-sigmoid bone was removed. Wooden wedges of 1,5 mm in thickness were incrementally positioned in the resection cavity until an additional wedge threatened to decrease the SS patency. Care was taken to keep the superior petrosal sinus intact. This manoeuvre is visualised in *figure 2*. The last procedure (TL-C) was performed virtually since it was deemed inaccurate to analyse the resection cavity after the retrosigmoid bone removal, which would likely result in unbridled amounts of dorsal mobilisation. To virtually perform this procedure, the 3D dimensional model of the TL-S was modified such that the intersection of the posterior border of the SS and dura was used as the most anteriorly located part of the sinus during TL-C. Thus, this virtual model assumes the walls of a collapsed sinus will lay completely flat along its posterior surface in line with the dura.

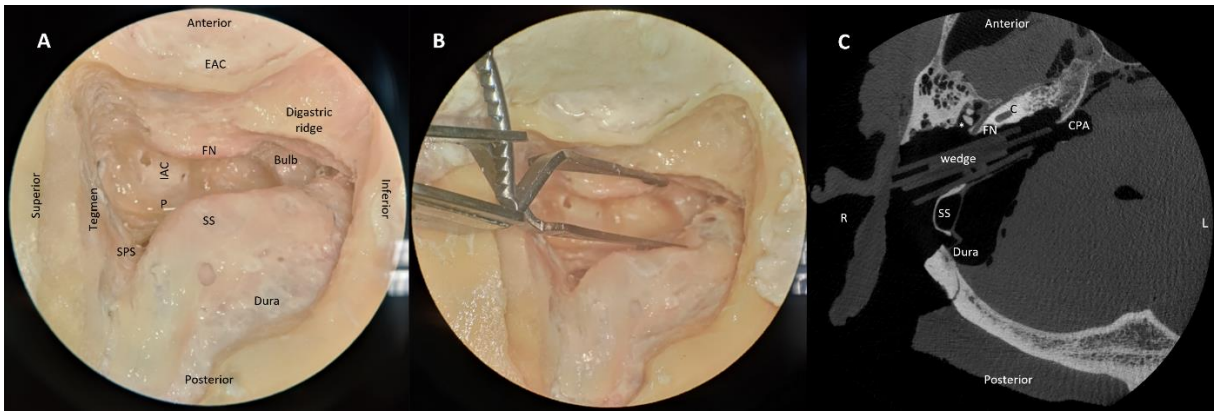

Figure 2: Lateral view of a right sided translabyrinthine approach without (A) and with (B) retraction of the sinus, and transversal post-operative (TL-R) CT-scan with wooden wedges in the resection

cavity (C). Note that the SS remains patent during retraction. *Legend: EAC = external auditory canal, FN = fascial nerve, IAC = internal auditory canal, Bulb = jugular bulb, P = porus acusticus internus, SS = sigmoid sinus, SPS = superior petrosal sinus, C = cochlea, * = incus, CPA = cerebellopontine angle.*

2.3. Exposure quantification

To accurately portray the exposure multiple parameters were defined: surgical freedom, field of view, and angle of attack. Each provides a quantification of different element that only on aggregate can meaningly inform a surgeon on the expected exposure and ease of resectability.

2.3.1. Surgical Freedom

The 'surgical freedom' (SF) was defined as the area of the two-dimensional plane at the level of the craniotomy through which surgical instruments can be inserted towards a specific target of interest. This objective quantification technique is based on a refinement of the conical solid method previously used by Schwartz et al. (11). D'Ambrosio et al. improved on the accuracy of this area by including a sophisticated model in which unobstructed 'lines of sight' from the target to a specific anatomical point at craniotomy were drawn. When an oblique plane was generated at the level of the craniotomy, the intersection of the lines with the plane allowed the formation of various triangles of which the area could be calculated (2, 13). This method allows for measurement of irregular areas, with the benefit of quantifying where the most benefit from the procedure will be received (i.e., which triangle) Furthermore, it can incorporate the concept 'depth till target' in the assessment.

In this study, the midpoint on the most proximal IAC surface was used as the primary target point. Although not the same, this point (P) projects directly above the internal acoustic porus. Lines of sight originating from P were placed in such a way that they visually most accurately conformed with the observed resection cavity, instead of using fixed anatomical points. Given that the aim of SF is quantification of an irregularly shaped area, and shape of the posterior border changes with retraction, different points along this border potentially represented the curvature of this shape more accurately than fixed translated anatomical points. A total of 6 lines were cast from the target point. Line 1 was placed one the most anterior part of the SS directly above (lateral to) the middle of the IAC; Line 2 was placed as far superior-posteriorly until either the sinodural angle or the tegmen was encountered ; Line 3 was placed most superior-anteriorly in the craniotomy; Line 4 was placed above (lateral to) the antero-lateral part of the IAC until either fascial nerve or the craniotomy was encountered; Line 5 was placed as far inferior-anteriorly on the craniotomy or until the fascial nerve was encountered; Line 6 was placed as far inferior-posteriorly on the craniotomy or until the SS was encountered.

An oblique plane was generated in the model which intersected both the edges of the craniotomy and the six generated lines. The points of intersection between the oblique plane and the six projected lines were identified and four triangles generated, connecting all points of intersection (13). Triangles A (points 1,2,4) and B (2,3,4) represent the surgical freedom to the superior aspect of the IAC and higher cranial nerves. Triangles C (4,5,6) and D (1,4,6) represent the inferior aspect of the IAC and lower cranial nerves. The areas of these triangles were calculated with Heron's formula. Overall surgical freedom was attained by the sum of these triangle area's (mm^2). See *figure 3* for the acquisition of SF.

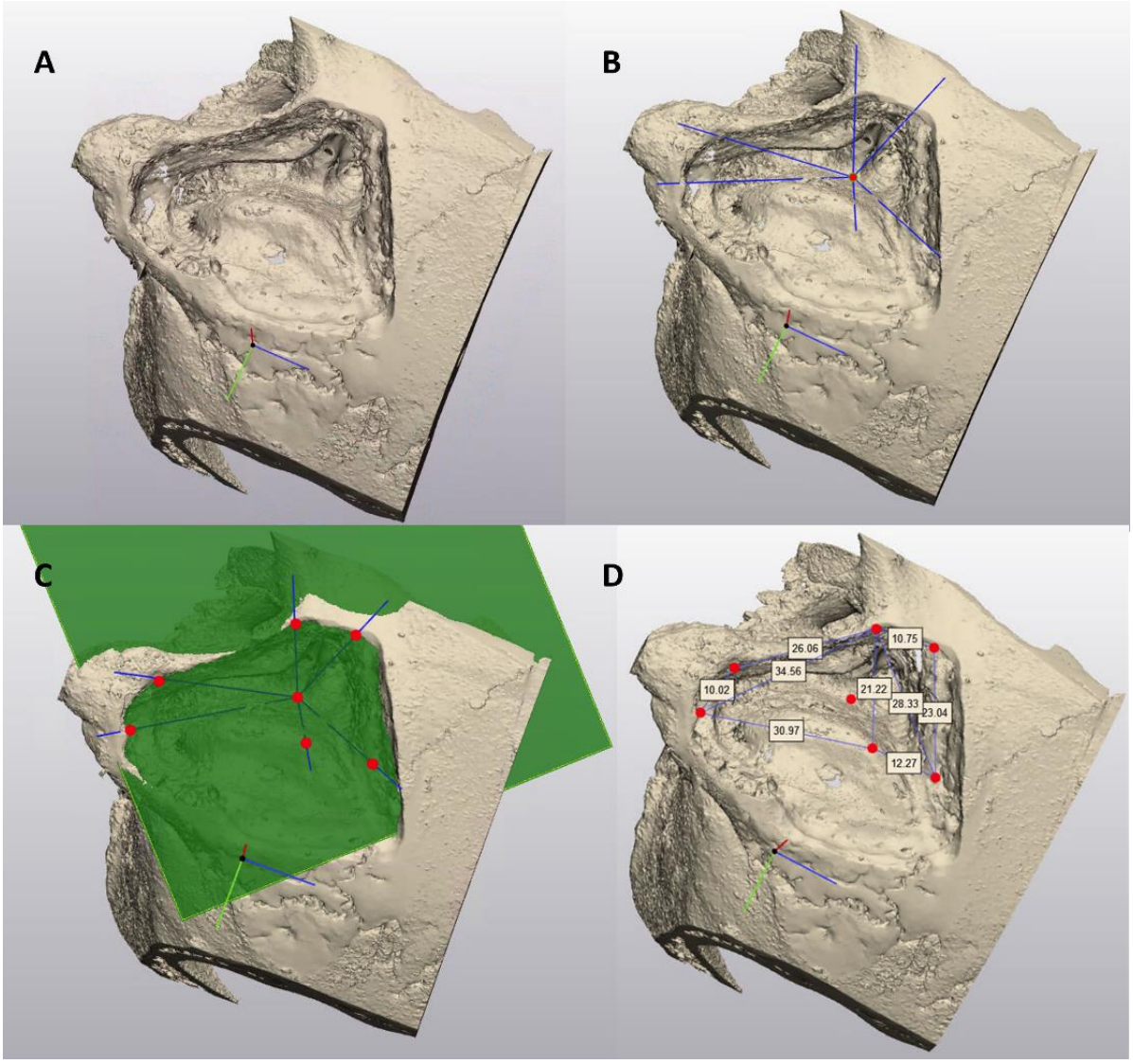

Figure 3: Acquisition of surgical freedom. (A) Dorsolateral view of a 3D model after left sided TL-S. (B) Six lines of sight originating from the porus. (C) Marking the intersection of these lines with the craniotomy plane. (D) Measured distances between those intersecting points.

2.3.2. Exposure Angle

Whereas the surgical freedom concerns itself with the available space to use instruments in, 'exposure angle' (EA) provides information about the mobility of those instruments. The EA is defined as the angle that a straight instrument could theoretically make in the transverse plane between the SS and the fascial nerve within the borders of the craniotomy. For the purpose of this study, the transverse plane is defined as a plane parallel to the surface of the tegmen. Although, the tegmen does not completely lay parallel to the genuine transverse plane, it is, in contrast to the CT-scan's transverse plane, consistent across different post-procedures CT-scans, and thus preferred. To find the EA, the angle between the following two straight lines in this plane is calculated. Firstly, the most horizontal line shearing the lateral part of the SS and the medial part of the fascial nerve is generated. Secondly, the most horizontal line shearing the medial part of the SS and the anterior craniotomy border is generated. The more acute this angle is, the less antero-posterior mobility there is. When the EA

increases during SS retraction, the space antero-medial to the fascial nerve enlarges, resulting in greater accessibility to the distal portion of the IAC.

Since the relative position as well as the absolute distance between the fascial nerve, the SS, and CPA varies in both the medial-lateral and the anterior-posterior direction, multiple EA measurements are required to portray the exposure more accurately. The EA is calculated in the transverse plane at the level of the midpoint on the most proximal IAC surface, i.e., point P (EA-IAC). Furthermore, the EA is calculated at the level of the superior portion of the jugular bulb (EA-IAC). The former is chosen to provide information regarding exposure of the IAC. The latter is chosen because the superior portion of the jugular bulb is deemed the most inferior edge of the resection medial to the fascial nerve. No EA is calculated superior of the IAC since the facial nerve shortly thereafter relays through its the first genu and into the IAC itself.

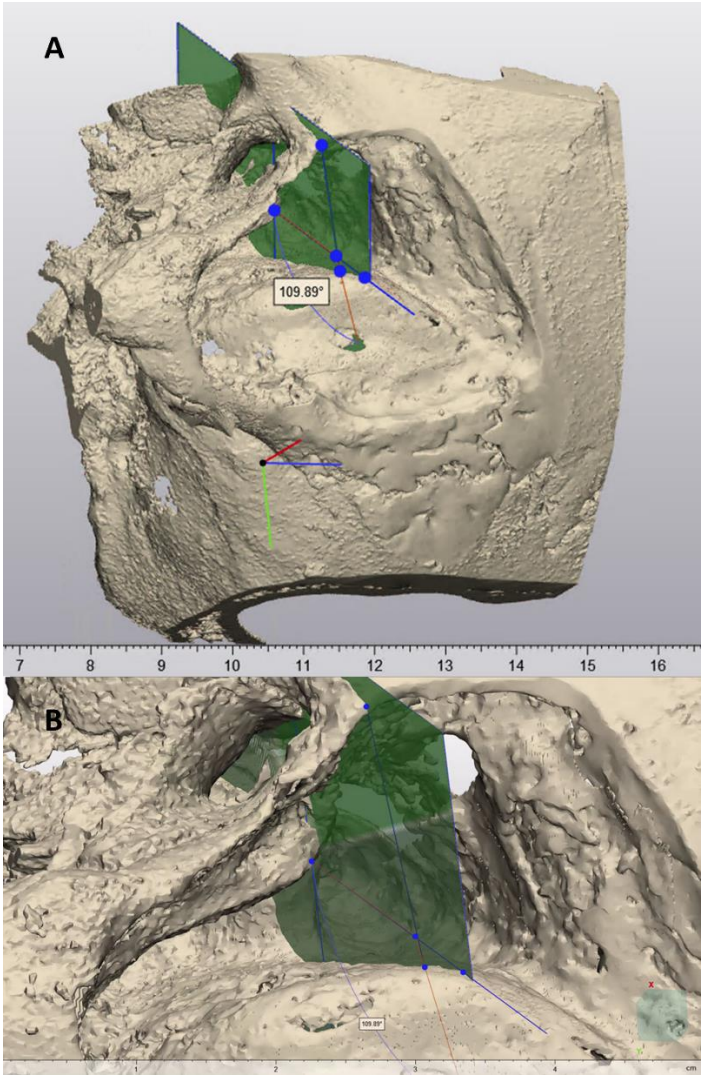

Figure 4: Acquisition of the exposure angle at the level of the IAC at various magnification from an inferior-lateral view. The angle at the intersection between two lines in the transverse plane originating from the craniotomy and the medial part of the fascial nerve shearing respectively the inferior and superior surface of the sigmoid sinus.

2.3.3. Angle of Attack / Approach Angle

The 'angle of attack' is defined as the angle between a straight line in the transverse plane from the SS to the midpoint on the proximal IAC surface (point P) and a straight line over middle of the IAC to its most anterolateral part. A 90-degree angle would entail a straight top-down approach, while a more acute angle (< 90 degrees) constrains the approach more anteriorly. An obtuse angle (> 90 degrees) allows a more posterior approach in conjunction with an anterior approach.

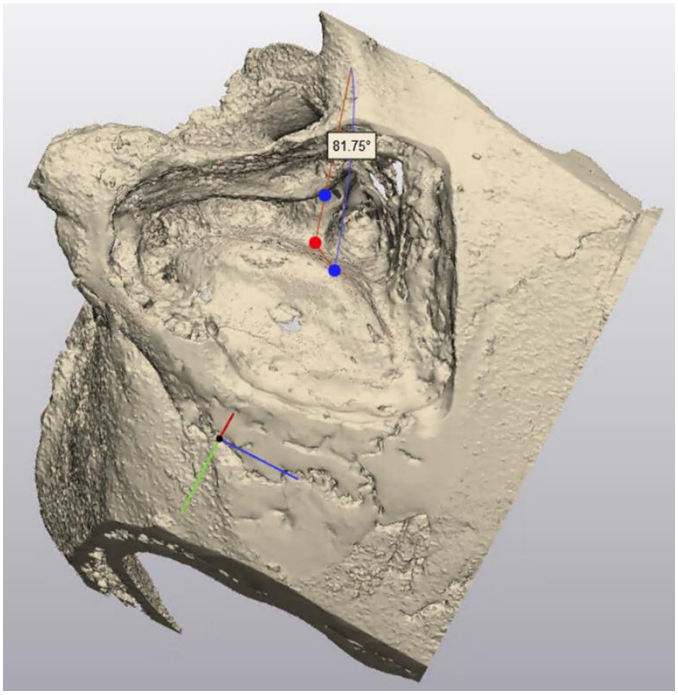

Figure 5: Acquisition of the angle of attack. The angle between the line over the surface of the IAC and a line from the sinus to the porus.

2.4. Statistical analysis

Power analyses were performed to estimate the sample size required to detect a difference in exposure of 15% or greater ($\alpha = 0.05$, power = 0.9), resulting in a recommended per group sample size of 9 to 10 depending on the specific formulas. Effect size and power was estimated based on previous anatomical skull base studies (2, 3, 8, 13). A two-tailed paired T-test (p_2) was used to determine statistical significance in the cases which compared TL-R and TL-C. However, due to the nature of the manoeuvre and clinical experience, any amount of sigmoid sinus retraction will increase the exposure when compared to TL-S; therefore, a one-tailed paired T-test (p_1) is preferred to determine statistical significance in cases which compared either TL-R or TL-C to TL-S. In all cases, $p < 0,05$ was considered significant. Microsoft Excel 2016 was used for data management. All statistical tests were performed in SPSS v28.

3. Results

3.1. Specimen preparation and characteristics

In all 12 temporal bones a translabyrinthine proper resection was achieved with exposure of the IAC. There were two cases (16,7%) of a high jugular bulb in which the superior aspect of the bulb projected over or touched the inferior border of the IAC (resp. specimen 4L, and 5R). A total of two temporal bones (spec. 1R and 6L) were excluded from the final analysis resulting in the study of 10 specimens. The former due to a prematurely collapsed SS after TL-S dissection. The latter due to a significant compression at the distal part of the SS on the post-TL-R CT-scan; thus, not securing sinus patency.

The pre-sigmoid depth was defined as the distance between the porus and the medial border of the SS. This depth (mean: 25 mm, range: 15-38 mm, SD: 5,8) did not statically significantly ($p_2 =$ 0,052) change after retraction of the SS during TL-R when compared to TL-S. The area of the pre-sigmoid dura, which is approximated by constructing a trapezoid with a medial base between the jugular bulb and the tegmen, a lateral base anterior to the vertical part of the SS, and the pre-sigmoid depth, ranged from 283 to 776 mm^2 (mean: 413 mm^2, SD: 151).

3.2. Surgical freedom

When retraction of the SS was performed during TL-R, surgical freedom increased by a mean of 41% (range: 9-92%, SD: 28) when compared to no retraction (TL-S). Collapsing the SS in TL-C provided a mean increase of 52% (range: 19-95%, SD: 22) compared to TL-S. In some specimens, the TL-R provided a greater SF than the TL-C; however, on average in increase of 10% (range: -10–30%, SD: 12) in favour of the TL-C is observed when compared to TL-R. *Figure 6* provides the SF stratified by specimen. See *figure 7* for the spread and mean of provided SF stratified by procedure. A statistically significant difference in mean surgical freedom between both TL-R (165 ± 72 mm^2, $p_1 < 0,01$) or TL-C (227 ± 84 mm^2, $p_1 < 0,01$) and TL-S was observed. Also, the difference in mean surgical freedom between TL-C and TL-R (62 ± 77 mm^2, $p_2 = 0,03$) was statistically significant.

Of the triangles used to calculate SF, the area of triangles A and D, projecting respectively superiorly and inferiorly above the (proximal) IAC, were most affected by the retraction with a mean increased percentage of 55% and 39% respectively. Triangles B and C increased on average 24% and 27% respectively.

Pearson correlation analysis of the pre-sigmoid area and surgical freedom after TL-S showed a high positive correlation ($r = 0,67$, $p_2 = 0,033$). Furthermore, both pre-sigmoid area ($r = -0,64$, $p_2 = 0,047$) and pre-sigmoid depth ($r = -0,70$, $p_2 = 0,024$) showed a high negative correlation with the percentage of increased surgical freedom when comparing TL-C with TL-S. No correlation between TL-R surgical freedom and pre-sigmoid area or depth was statistically significant.

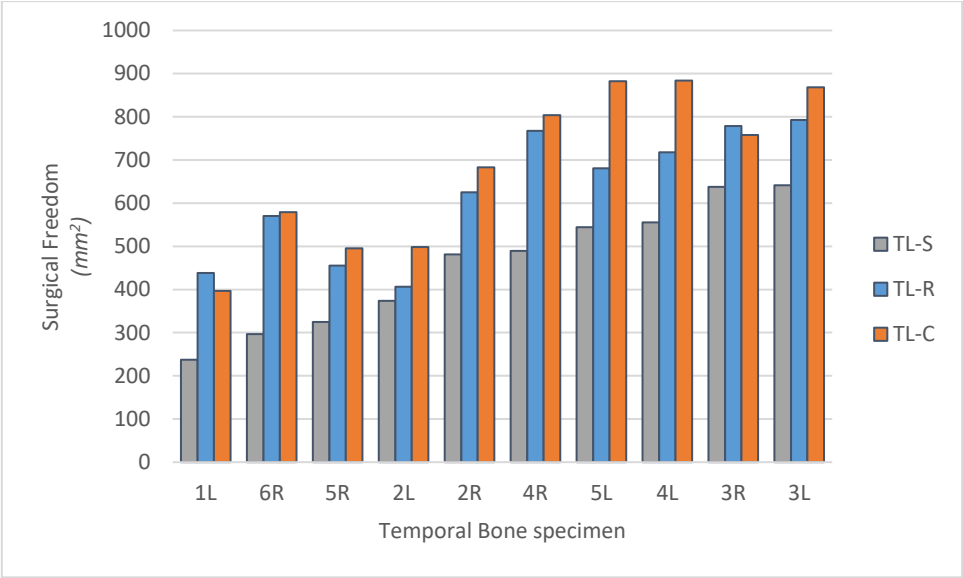

Figure 6: Surgical freedom (mm^2) stratified by procedure and specimen, and ranked by TL-S.

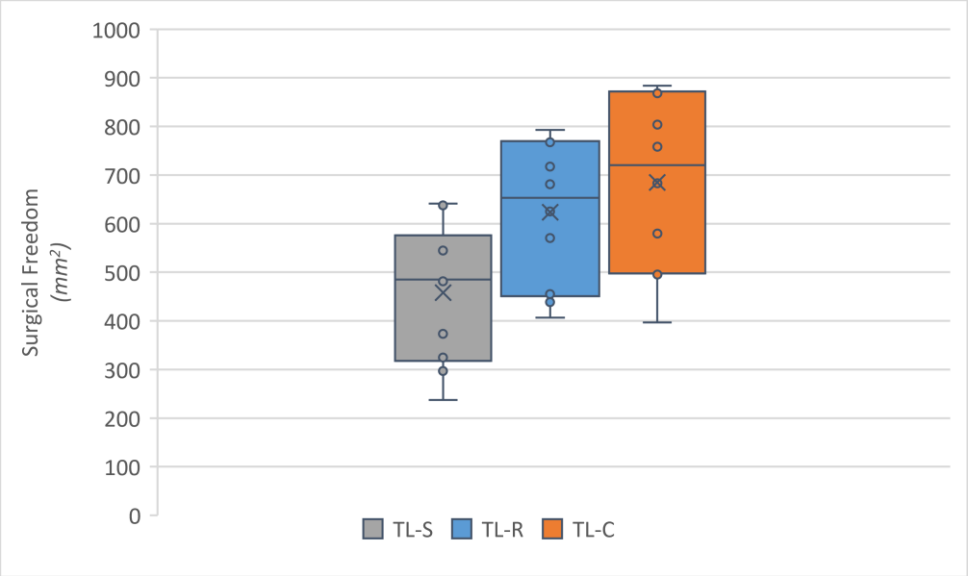

Figure 7: Boxplot of surgical freedom (mm^2) stratified by procedure.

3.3. Exposure angle

The mean exposure angle above the IAC statistically significantly increased in both the TL-R (14 ± 11°, $p_1 = 0{,}001$) and TL-C R (13 ± 8°, $p_1 < 0{,}001$) when compared to TL-S. The mean exposure angle above the jugular bulb statistically significantly increased in both the TL-R (15 ± 16°, $p_1 = 0{,}006$) and TL-C (14 ± 10°, $p_1 = 0{,}001$) when compared to TL-S. There was no statistically significant difference in the exposure angles when comparing TL-C to TL-R at both the level of the IAC (-0,5 ± 6°, $p_2 = 0{,}82$) as well as the jugular bulb (-2 ± 17°, $p_2 = 0{,}78$). Both absolute exposure angles as well as the percentage increased are shown in *Table 1*.

Pearson correlation analysis of the exposure angle in either TL-S, TL-R or TL-C, and pre-sigmoid area or depth did not provide significant correlations.

3.4. Angle of attack

The mean angle of attack increased at each successive step of the resection from 67° (range: 49-88°, SD: 13), to 76° (range: 60-103°, SD 13), and 84° (range: 60-103°, SD: 13) in TL-S, TL-R, and TL-C respectively. These results are shown in *Table 1*. The difference in mean angle of attack in TL-R (9 ± 4°, $p_1 < 0{,}001$) and TL-C (17 ± 5°, $p_1 < 0{,}001$) was statically significant when compared to TL-S. The difference in mean angle of attack when comparing TL-C to TL-R was 8 ± 6° ($p_2 = 0{,}003$).

Pearson correlation analysis of the angle of attack in either TL-S, TL-R or TL-C, and pre-sigmoid area or depth did not provide significant correlations.

Table 1: Quantification of the mean exposure angle and angle of attack with various sigmoid sinus positions

Surgical approach	**Exposure angle**		**Angle of attack**
	IAC	Jugular bulb	IAC
TL-S	94 ° ± 14	78 ° ± 14	67 ° ± 13
TL-R	108 ° ± 10	93 ° ± 9	76 ° ± 13
TL-C	108 ° ± 9	91 ° ± 18	84 ° ± 13
% increased			
TL-R [a]	16 % ± 14	25 % ± 31	14 % ± 8
TL-C [a]	16 % ± 10	18 % ± 13	26 % ± 11
TL-Δ [b]	0 % ± 6 [C]	-1 % ± 18 [C]	11 % ± 9
Abbreviations: IAC, Internal auditory canal; TL-S, translabyrinthine without sinus retraction; TL-R, translabyrinthine with retracted patent sinus; TL-C, translabyrinthine with collapsed sinus; ±, standard deviation.		[a] Increased percentage of degrees compared to same specimen TL-S. [b] Increased percentage of degrees of TL-C compared to same specimen TL-R. [c] Statistical significancy was not reached (p>0,05).	

4. Discussion

4.1. Technical and methodologic consideration

Various methods have been used to quantify exposure ranging from stereophotographic measurements of dissected cadaveric specimens (12, 16) to complete digital simulation of the procedure (13). More recently, cadaveric dissection and variables calculated from neuro-navigation coordinates has gained popularity (6, 9, 14, 17, 28). Similarly, our technique used real world dissection and a digital representation of this resection cavity to quantify the exposure. Creating a high-resolution 3D model of this cavity enabled an even more meticulous process to quantify the outcomes in a reproducible manner. Furthermore, it allowed for measurement and representation of angles and distances which would not easily be acquired due to physical constraints. Because of this, a strength of this study has become the use of multiple outcome measures of exposure.

However, this method had a significant constraint in that it was only possible to measure substances that would show up on the CT-scan. For this reason, it was chosen to leave a thin bony covering on areas of interests. The measurement error as result of the thickness of this covering is, we believe, negligible and might even improve reproducibility since it reduces the inherent mobility soft tissue has and provides a recognizable surface across the procedures. Nevertheless, this limited mobility might have constrained the SS during retraction. Similarly, the pre-sigmoid dura, when compared to a situation in which the dura is opened to access the CPA, probably constrained the movement of the SS. This hypothesis is supported by the lack of change in pre-sigmoid depth between TL-S and TL-R.

Furthermore, a cadaveric model does not replicate the anatomical distortion and changes in tissue characteristics caused by CPA-pathology (6). Although, the use of fresh frozen instead of formaldehyde-fixated specimens provided a more accurate representation of the mobility, the lack of intracranial pressure could have influenced the results. However, as Martins Coelho Jr. et al. (2023) notes, ‘the eventual widening of the anatomical corridor by a substantial tumour, implies both greater instrument manoeuvrability and better visualisation of the [CPA]’ (6). Thus, we expect that our results on the maximally afforded additional exposure due to retraction of this sinus is likely the lower limit.

The position of the SS during TL-C and the performed TL proper in patients can differ in various amount. In this study it is assumed that the collapsed position of the sinus remains stationary. However, based on the surgeon’s preference, various amounts of retro-mobilization of the collapsed SS might be performed (20). This partially compresses, but not as much as during a retrosigmoid approach, the cerebellum providing an even greater exposure than out TL-C suggested. In doing so, the difference between TL-S and TL-C increases. However, greater retrosigmoid dissection than is provided in these specimens might be required. It is plausible that the surgical exposure in TL-R will similarly increase with greater retrosigmoid dissection.

4.2. Quantification of surgical exposure

Although the surgical exposure seemed to increase the most with the collapsed SS (TL-C), retracting a skeletonized SS conserves patency in exchange for approximately 10% of surgical freedom and 8 degrees in the angle of attack; there seemed to be no statistically significant difference in exposure angles over the IAC and jugular bulb.

The simultaneous changed angle of attack in combination with the unchanged exposure angles, seems ad hoc contradictory. One hypothesis for this phenomenon could be that the effect size is smaller than anticipated, since the position of the sinus was fixed to the porus by the pre-sigmoid dura. Thus, the

mobility of the sinus is not (merely) a posterior translation, but also medial translation, rotating around the porus by its dural-tether. This motion would alter the shearing lines required for exposure angle measurement less than a pure posterior translation. Another hypothesis could be the assumed change in shape of the SS lumen during the TL-C: from a mostly round shape in TL-S and TL-R, to a flat shape in line with the dura. This change in shape would impact the anterior border of the SS, relevant to angle of attack, more than the medial and lateral borders, which are relevant to approach angle. A third explanation could be that, because the intersection of the two shearing lines in exposure angle is relatively close to the SS itself, the small measurement error is amplified.

The large spread of provide exposures across the specimens would classically be considered a negative in quantitative anatomical studies, however since this study sequentially performed all procedures on each specimen, this should be considered one of its strengths; it evaluated specimens with sparse surgical freedom ranging from 250 mm^2 up to a generous 650 mm^2 after TL-S. The pre-sigmoid area was significantly correlated to the surgical freedom post TL-S. Furthermore, an inverse correlation was observed with the percentage increased surgical freedom after collapsing the sinus. In other words, the greater the distance between the porus and the sinus, the less ancillary exposure is gained by collapsing the sinus. Thus, retracting a skeletonized sinus might in those capacious cases result in satisfactory exposure. This claim is substantiated by the propinquity in the boxplot between the surgical freedom of TL-R and TL-S, and the fact that the top 40% of TL-R surgical freedom is greater than the bottom 50% of TL-C.

4.3. Practical considerations and future perspective

A limitation of using this model, is the absence of venous pressure which would aid in keeping the SS patent. The overall aim of retracting a skeletonized sinus was to ensure patency. During this study patency was violated in one specimen during the retraction. To mobilize the sinus, careful dissection of the peri-sinoid bone is coveted. However, during the retraction, depending on the specific thickness of the skeletonized bone, some buckling of this bone might appear. Due to the round shape and direction of the compression the bony plates pushed outwards, thus not endangering the SS superficial vessel wall. To minimize this probability, a relatively conservative skeletonization should be aimed for, leaving ample bone on the sinus. This is especially important on the anterolateral walls of the sinus to benefit from the Roman bridge effect caused by the rounded shape during retraction, and distally near the jugular bulb since this part seemed to be the least compliant to this direction of motion.

Augmented and mixed reality (AR and MR) applied to neuro- and skull base surgery has become a promising research interest. Fick et al. (2021) showed the reliability, accuracy, and speed of AR in clinical neurosurgical practice and its ability to fully automatic segment tumours (29). Pennacchietti et al. (2021) demonstrated the additional benefit of using AR in endoscopic-assisted skull base surgery (7). The benefits of this technology reaches beyond education and pre-operative planning, and can provide simultaneous multisource information to even experienced surgeons (30). Likewise, mixed reality, in which the information is not only projected over the object, but also provides interactive virtual data, could in the future be helpful in estimating how exposure will change with a dynamic mobilization of the soft tissue anatomy. Studies like this one, that quantify not only static exposure, but also the compliance of structures could be valuable to these developments. Ideally, the operating team could model and visualise in 3D the expected exposure in the CPA through the petrous bone using various retractions of the sigmoid sinus using patient specific data.

5. Conclusions

This study presented data from three sequentially performed degrees of sigmoid sinus retraction during the translabyrinthine proper approach. While in most cases the exposure is the greatest when the sigmoid sinus is collapsed, in some cases the exposure granted by retracting a skeletonized sinus is at least equal to other cases in which the sinus is fully collapsed. It is therefore concluded that with careful patient selection a translabyrinthine resection in which the skeletonized sigmoid sinus is retracted, is indeed feasible while providing sufficient exposure. However, further research is necessary to evaluate the translatability of manoeuvre from cadaveric specimens to a clinical setting.

6. Acknowledgements and disclosures

This study was performed under the supervision and guidance of H.G.X.M. Thomeer (ENT surgeon, UMC Utrecht) and E.H.J. Voormolen (neurosurgeon, UMC Utrecht). There were no conflicts of interest. No funding was received for this study. I would like to thank R.A.W.L. Bleys and M. Rondhuis (Department of Anatomy, UMC Utrecht) for the procurement and selection of the specimens. Furthermore, special thanks to Mijs Buter for explaining and aiding in the use of the 3D modelling software.

Bibliography

1. Figueiredo EG, Deshmukh P, Zabramski JM, Preul MC, Crawford NR, Siwanuwatn R, et al. Quantitative anatomic study of three surgical approaches to the anterior communicating artery complex. Neurosurgery. 2005;56(2 Suppl):397-405; discussion 397-405.
2. Gonzalez LF, Crawford NR, Horgan MA, Deshmukh P, Zabramski JM, Spetzler RF. Working area and angle of attack in three cranial base approaches: pterional, orbitozygomatic, and maxillary extension of the orbitozygomatic approach. Neurosurgery. 2002;50(3):550-5; discussion 5-7.
3. Horgan MA, Anderson GJ, Kellogg JX, Schwartz MS, Spektor S, McMenomey SO, et al. Classification and quantification of the petrosal approach to the petroclival region. J Neurosurg. 2000;93(1):108-12.
4. Tang CT, Kurozumi K, Pillai P, Filipce V, Chiocca EA, Ammirati M. Quantitative analysis of surgical exposure and maneuverability associated with the endoscope and the microscope in the retrosigmoid and various posterior petrosectomy approaches to the petroclival region using computer tomograpy-based frameless stereotaxy. A cadaveric study. Clin Neurol Neurosurg. 2013;115(7):1058-62.
5. de Melo JOJ, Klescoski JJ, Nunes CF, Cabral GA, Lapenta MA, Landeiro JA. Predicting the presigmoid retrolabyrinthine space using a sigmoid sinus tomography classification: A cadaveric study. Surg Neurol Int. 2014;5:131.
6. Martins Coelho VP, Jr., Saquy Rassi M, Colli BO. Retrosigmoid versus Retrolabyrinthine Posterior Petrosal Route to the Petroclival Area: Quantitative Assessment of Endoscope-Assisted Approaches and Correlations with Morphometric Features. World Neurosurg. 2023;173:e462-e71.
7. Pennacchietti V, Stoelzel K, Tietze A, Lankes E, Schaumann A, Uecker FC, et al. First experience with augmented reality neuronavigation in endoscopic assisted midline skull base pathologies in children. Childs Nerv Syst. 2021;37(5):1525-34.
8. Muelleman TJ, Maxwell AK, Peng KA, Brackmann DE, Lekovic GP, Mehta GU. Anatomic Assessment of the Limits of an Endoscopically Assisted Retrolabyrinthine Approach to the Internal Auditory Canal. J Neurol Surg B Skull Base. 2021;82(Suppl 3):e184-e9.

9. Saraceno G, Agosti E, Qiu J, Buffoli B, Ferrari M, Raffetti E, et al. Quantitative Anatomical Comparison of Anterior, Anterolateral and Lateral, Microsurgical and Endoscopic Approaches to the Middle Cranial Fossa. World Neurosurgery. 2020;134:e682-e730.
10. Figueiredo EG, Beer-Furlan A, Nakaji P, Crawford N, Welling LC, Ribas EC, et al. The Role of Endoscopic Assistance in Ambient Cistern Surgery: Analysis of Four Surgical Approaches. World Neurosurg. 2015;84(6):1907-15.
11. Schwartz MS, Anderson GJ, Horgan MA, Kellogg JX, McMenomey SO, Delashaw JB, Jr. Quantification of increased exposure resulting from orbital rim and orbitozygomatic osteotomy via the frontotemporal transsylvian approach. J Neurosurg. 1999;91(6):1020-6.
12. Schwartz MS, Anderson GJ, Horgan MA, Kellogg JX, McMenomey SO, Delashaw JB. Quantification of increased exposure resulting from orbital rim and orbitozygomatic osteotomy via the frontotemporal transsylvian approach. Journal of Neurosurgery. 1999;91(6):1020-6.
13. D'Ambrosio AL, Mocco J, Hankinson TC, Bruce JN, van Loveren HR. Quantification of the frontotemporal orbitozygomatic approach using a three-dimensional visualization and modeling application. Neurosurgery. 2008;62(3 Suppl 1):251-60; discussion 60-1.
14. Yagmurlu K, Safavi-Abbasi S, Belykh E, Kalani MYS, Nakaji P, Rhoton AL, Jr., et al. Quantitative anatomical analysis and clinical experience with mini-pterional and mini-orbitozygomatic approaches for intracranial aneurysm surgery. J Neurosurg. 2017;127(3):646-59.
15. da Silva SA, Yamaki VN, Solla DJF, Andrade AF, Teixeira MJ, Spetzler RF, et al. Pterional, Pretemporal, and Orbitozygomatic Approaches: Anatomic and Comparative Study. World Neurosurg. 2019;121:e398-e403.
16. Siwanuwatn R, Deshmukh P, Figueiredo EG, Crawford NR, Spetzler RF, Preul MC. Quantitative analysis of the working area and angle of attack for the retrosigmoid, combined petrosal, and transcochlear approaches to the petroclival region. Journal of Neurosurgery JNS. 2006;104(1):137-42.
17. Serioli S, Agosti E, Buffoli B, Raffetti E, Alexander AY, Salgado-López L, et al. Microsurgical transcranial approaches to the posterior surface of petrosal portion of the temporal bone: quantitative analysis of surgical volumes and exposed areas. Neurosurg Rev. 2023;46(1):48.
18. Luo Z, Zhao P, Yang K, Liu Y, Zhang Y, Liu H. The Microsurgical Anatomy of the Modified Presigmoid Trans-Partial Bony Labyrinth Approach. J Craniofac Surg. 2015;26(5):1619-23.
19. Hoz SS, Palmisciano P, Albairmani SS, Kaye J, Muthana A, Johnson MD, et al. A proposed classification system for presigmoid approaches: a scoping review. J Neurosurg. 2023:1-7.
20. Jackler RK. Atlas of Skull Base Surgery & Neurotology: Thieme; 2009. Available from: https://skullbasesurgeryatlas.stanford.edu/illustrations-of-skull-base-surgery-and-neurotology/lateral-approaches-to-the-internal-auditory-canal-and-cerebellopontine-angle/translabyrinthine-approach/#.
21. Fatima N, Barnard ZR, Maxwell AK, Muelleman TJ, Slattery WH, Mehta GU, et al. The Role of Intra-Operative Duplex Ultrasonography Following Translabyrinthine Approach for Vestibular Schwannoma. Front Surg. 2022;9:853704.
22. Song Y, Ayoub N, Chen JX, Alyono JC, Welling DB. Pulmonary Embolism and Sigmoid Sinus Thrombosis After Translabyrinthine Vestibular Schwannoma Resection: A Retrospective Case Series. Ann Otol Rhinol Laryngol. 2022;131(6):683-9.
23. Freeman MH, Cass ND, Berndt DM, Kloosterman N, Poulos EA, Perkins EL, et al. Association of Postoperative Sigmoid Sinus Occlusion and Cerebrospinal Fluid Leak in Translabyrinthine Surgery. Otolaryngol Head Neck Surg. 2023;168(3):435-42.
24. Shew M, Kavookjian H, Dahlstrom K, Muelleman T, Lin J, Camarata P, et al. Incidence and Risk Factors for Sigmoid Venous Thrombosis Following CPA Tumor Resection. Otol Neurotol. 2018;39(5):e376-e80.
25. Arnone GD, Kunigelis KE, Gurau A, Coulter I, Thompson J, Youssef AS. Acute Sigmoid Sinus Compromise Following Skull Base Procedures: Is a "Laissez-Faire" Approach Best? J Neurol Surg B Skull Base. 2021;82(6):652-8.

26. Ziegler A, El-Kouri N, Dymon Z, Serrano D, Bashir M, Anderson D, et al. Sigmoid Sinus Patency following Vestibular Schwannoma Resection via Retrosigmoid versus Translabyrinthine Approach. J Neurol Surg B Skull Base. 2021;82(4):461-5.
27. Brahimaj BC, Beer-Furlan A, Crawford F, Nunna R, Urban M, Wu G, et al. Dural Venous Sinus Thrombosis after Vestibular Schwannoma Surgery: The Anticoagulation Dilemma. J Neurol Surg B Skull Base. 2021;82(Suppl 3):e3-e8.
28. Kwon SM, Na MK, Choi KS, Bang JH, Byoun HS, Han H, et al. Comparative Cadaveric Analysis for Surgical Corridor and Maneuverability: Far-Lateral Approach and Its Transcondylar Extension. World Neurosurg. 2021;146:e979-e84.
29. Fick T, van Doormaal JAM, Tosic L, van Zoest RJ, Meulstee JW, Hoving EW, et al. Fully automatic brain tumor segmentation for 3D evaluation in augmented reality. Neurosurg Focus. 2021;51(2):E14.
30. Vervoorn MT, Wulfse M, Van Doormaal TPC, Ruurda JP, Van der Kaaij NP, De Heer LM. Mixed Reality in Modern Surgical and Interventional Practice: Narrative Review of the Literature. JMIR Serious Games. 2023;11:e41297.